Available online at www.sciencedirect.com
ScienceDirect
St. Petersburg Polytechnical University Journal: Physics and Mathematics 2 (2016) 181–187
www.elsevier.com/locate/spjpm

An analysis of the high-temperature phase structure of multiferroic solid solutions of the PFW–PT

Aleksandr A. Naberezhnov[a,b], Ivan A. Dolgakov[b,*], Mikhael Tovar[c], Olga A. Alekseeva[b], Sergey B. Vakhrushev[a,d]

[a] *Ioffe Institute, 26 Politekhnicheskaya St., St. Petersburg, 194021, Russian Federation*
[b] *Peter the Great St. Petersburg Polytechnic University, 29 Politekhnicheskaya St., St. Petersburg, 195251, Russian Federation*
[c] *Helmholtz-Zentrum Berlin für Materialien und Energie GmbH, Glienicker St., 14109 Berlin, Germany*
[d] *St. Petersburg State University, 1 Ul'yanovskaya St., Petrodvorets, St. Petersburg, 195504, Russian Federation*

Available online 20 August 2016

Abstract

The temperature evolution of multiferroic solid solutions of the PFW–PT system, namely a $(1–x)Pb(Fe_{2/3}W_{1/3}O_3)–(x)PbTiO_3$ crystal structure where $x = 0$, 0.2, 0.3, has been studied by neutron powder diffraction in the region of the morphotropic phase boundary. The coexistence of cubic and tetragonal phases in the solutions with $x = 0.2$, 0.3 was found below $T = 259$ and 285 K, respectively. As a result of the data treatment, the atom coordinates, the occupation factors and the temperature dependences of cell parameters were determined in the cubic perovskite phase. The refinement of the crystal structure in terms of ideal perovskite exhibited anomalously large Debye–Waller factors for the lead cations, indicating the appearance of random static displacements of these cations from the ideal perovskite (0 0 0) position. Using the split-ion model we estimated the value of Pb static shifts (~0.1 Å) from their high-symmetry positions along the [1 1 0] direction. It was shown that these shifts decrease with increasing the $PbTiO_3$ concentration.

Keywords: Multiferroics; Crystalline structure; Neutron diffraction; Morphotropic phase boundary; Ferroelectrics-relaxors.

1. Introduction

Materials that simultaneously have ferroelectric and magnetic properties, especially at room temperature, have attracted considerable attention from researchers in the recent years. The crux of the matter is that the relationship between the electric and the magnetic subsystems in these materials is manifested in the form of magnetoelectric effects. This allows using the electric field to control the magnetic properties, and, vice versa, adjust the electrical properties by the magnetic field. The coexistence of ferroelectric and magnetic properties in single-phase materials and the possible connection between the two order parameters leads to an additional degree of freedom appearing when various devices are fabricated. Examples include devices

* Corresponding author.
E-mail addresses: alex.nabereznov@mail.ioffe.ru (A.A. Naberezhnov), dolgakovv@gmail.com (I.A. Dolgakov), tovar@helmholtz-berlin.de (M. Tovar), blackhole2010@yandex.ru (O.A. Alekseeva), s.vakhrushev@mail.ioffe.ru (S.B. Vakhrushev).

http://dx.doi.org/10.1016/j.spjpm.2016.08.005

for modulating the amplitudes, the polarization and the phases of optical waves, optical diodes, spin wave generators, frequency conversion devices. Additionally, it is possible to use the magnetoelectric interaction for switching (modulating) the electric polarization by the magnetic field.

The solid solution of the $PbFe_{2/3}W_{1/3}O_3$ type (PFW for short) is a relaxor ferroelectric with the $Pb(B'_{1-x}B''_x)O_3$ perovskite structure with non-isovalent substitution of ions at B site. Ref. [1] was the first to synthesize PFW and analyze its structure by X-ray crystallography. That study also determined the Curie temperature for this compound (183 K) and suggested the presence of antiferromagnetic properties (along with ferroelectric ones) associated with the presence of Fe^{3+} ions. Later, Refs. [2,3] found that the long-range antiferromagnetic order developed in PFW under temperatures below 363 K (the Néel temperature).

Ref. [4] proved that PFW possessed relaxor properties, i.e., that the temperature of the dielectric permittivity peak ε depended on the frequency and the presence of the frequency dispersion $\varepsilon(\omega,T)$ below the temperature of the peak ε. Ref. [5] established that adding the $PbTiO_3$ (PT) ferroelectric to PFW allowed to obtain a continuous series of solid (1–x)PFW–(x)PT solutions. A phase diagram was constructed on the basis of these studies, indicating that the Néel temperature decreased with an increase of the PT concentration, while the Curie temperature increased. This diagram also included a region in PFW–PT where the ferroelectric and the antiferromagnetic states coexisted.

The solid solutions in question were first studied by X-ray crystallography in [4] at room temperature for the values $x = 0$; 0.10; 0.20; 0.25; 0.30; 0.325; 0.35; 0.40; 0.60 and 0.80. The analysis of the diffraction patterns revealed that the sample exhibited a cubic phase at $0 < x < 0.25$. The dielectric spectroscopy results obtained in [4] revealed typical relaxor properties, such as the frequency dispersion of the dielectric permittivity peak and the failure of the Curie–Weiss law, in the (x, T) coordinates near the (0, 190) and (0.1, 220) points where the transition from cubic to pseudocubic phase occurs (Fig. 1).

The frequency dependence of the dielectric permittivity peak weakens substantially with an increase of x along the interphase boundary (between the cubic phase and any other), but at high temperatures, there are marked deviations from the Curie–Weiss law. The solution behaves like a normal ferroelectric near the (0.6; 500) point and above. More detailed (with respect to the lead titanate concentration) studies at

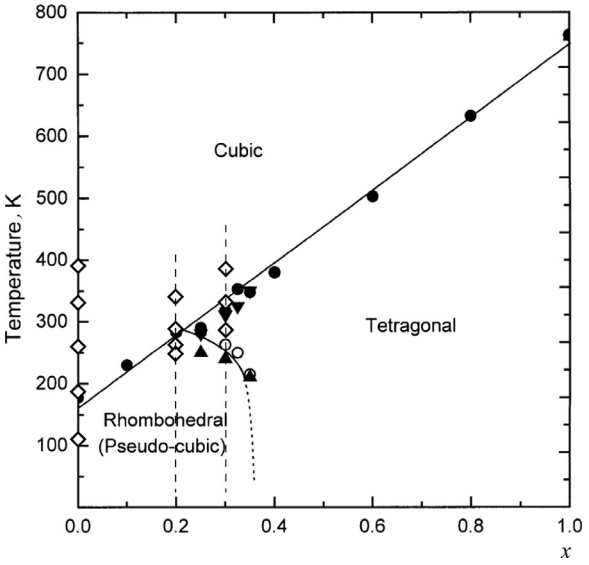

Fig. 1. Phase diagram of solid (1–x)PFW–(x)PT solutions from Ref. [4]. The diamonds mark the points where measurements were made in our experiment.

room temperature were conducted in [6] for solid (1–x)PFW–(x)PT solutions at $x = 0.0$; 0.10; 0.15; 0.20; 0.25; 0.27; 0.30; 0.31; 0.32; 0.35; 0.37; 0.40; 0.50 and 1.0. It was established that the cubic and the tetragonal phases coexisted in the $0.20 < x < 0.37$ region. The dependence for the percentage of these phases depending on x was also obtained. Ref. [4] constructed a phase diagram for (1–x)$Pb(Fe_{2/3}W_{1/3}O_3)$–(x)$PbTiO_3$ based on the data obtained by differential scanning calorimetry and by measuring the dielectric permittivity (see Fig. 1). It can be clearly seen that the temperature of the transition from the cubic phase (space group (SG) $Pm\bar{3}m$) into the pseudocubic one with the $R3m$ symmetry or the tetragonal one (SG $P4mm$) increases linearly with an increase of x. The pseudocubic phase is cubic with rhombohedral distortions of less than 0.01° [6]; it is in this phase that the compound exhibits relaxor properties. The tetragonal phase is normal ferroelectric. The region of the PT concentrations $0.25 < x < 0.35$ where different phases coexist is called the morphotropic phase boundary (MPB). Compounds of this type are known to exhibit the most interesting macroscopic properties, such as high values of dielectric permittivity, piezoelectric response, electrostriction, etc., exactly in the MPB region.

We should note that the past structural studies were carried out mainly at the same temperature for different compounds; consequently, the dependence of the phase percentage ratio on the temperature in the MPB

region, and the details of the structure temperature evolution in this region remained unexplored.

The goal of this contribution is to fill the existing gap in the structural studies. In the first stage, we have focused our attention on examining the features of the temperature evolution of the structure of the high-temperature phase of solid $(1–x)Pb(Fe_{2/3}W_{1/3}O_3)–(x)PbTiO_3$ solutions in the MPB region. Unlike previous studies, the composition–temperature phase diagram was scanned along the temperature axis (the vertical dashed lines in Fig. 1).

2. Samples and measurement procedure

The PFW and PFW–PT samples were fabricated by E.A. Dyadkina (Skripchenko) at the Voronezh State Technical University by the standard ceramic technology using double sintering [7]. $PbFe_{2/3}W_{1/3}O_3$ and $PbTiO_3$ powders were synthesized in advance at temperatures of 1050 and 920 K, respectively, in air for 3 h. The synthesized material was then thoroughly dry-milled and mixed in the required proportions. The resulting powder mixture was granulated. The final sintering stage was carried out at temperatures of 1170 and 1200 K for $x = 0.2$ and 0.3, respectively, also in air for 3 h. Next, the obtained ceramic samples were ground into fine ($\sim 1\,\mu$m) powders that were poured into cylindrical vanadium containers. The diffraction spectra were measured by a high-resolution E9 neutron diffractometer and a high-intensity E2 diffractometer (Helmholtz Zentrum Berlin (HZB), the BER II reactor). The incident neutron wavelength was 1.79 Å in the first case and 1.21 Å in the second case. The samples in vanadium containers were placed in a cryogenic oven that allowed performing measurements in the temperature range from 90 to 500 K; the temperature was maintained with a stability no worse than ±2 K. The resulting diffraction patterns were processed with the standard full profile analysis program FULLPROF [8].

3. Results and discussion

The first stage involved testing whether the samples obtained were actually solid PFW–PT solutions rather than a mechanical mixture of these compounds. Since it is known that the $Pb(Fe_{2/3}W_{1/3})O_3$ compound is in the cubic phase ($Pm\bar{3}m$) and $PbTiO_3$ is in the tetragonal phase ($P4mm$) in the high-temperature range (300–500 K), the diffraction profiles were described in a two-phase approximation within the mechanical mixture model. Data processing has revealed that the obtained diffraction patterns cannot be adequately described by the hypothesis of the mechanical mixture of the initial components, in particular, $R_{ft} = 76\%$ and $R_{fc} = 16\%$, where R_{ft} and R_{fc} are the R-factors for the tetragonal and the cubic phases, respectively. At the same time, using the model of the solid solution of stoichiometric composition in the cubic phase with the space group $Pm\bar{3}m$ lead to a significant improvement of the R-factor ($R_{fc} = 3.8\%$).

Fig. 2 shows a typical diffraction pattern for the (0.8)PFW–(0.2)PT compound, obtained at a temperature of 345 K. The dots represent the experimental results, and the lines the approximation of the experimental data within the model of the solid solution of stoichiometric composition. The line at the bottom of the figure is the residual between the approximation and the experimental data.

Primary analysis of the temperature evolution of the diffraction patterns identified two groups of peaks, $(h\,k\,l)$, for which at least two indices are different, and $(h\,h\,h)$, with fundamentally different temperature behavior: additional shoulders (or wings) emerging and subsequent splitting are observed with a decrease of temperature for the $(h\,k\,l)$ peaks, while the width and the shape of the $(h\,h\,h)$ peaks remain unchanged.

Fig. 3 shows as an example the temperature evolution of the (3 1 0) and (2 2 2) reflections of the solid solution of the $(1-x)$PFW–(x)PT compound at $x = 0.2$. For comparison, the same figure also shows the instrumental profile of the peak intensity, calculated for the temperature $T = 345$ K within the space group $Pm\bar{3}m$ without taking into account the size effects and the elastic stresses. The (3 1 0) peak was selected to represent the $(h\,k\,l)$ group, as it is located at large values of 2θ and therefore small changes in the structural factor lead to significant distortions of this reflection. The (2 2 2) peak was selected for comparison as a peak of the $(h\,h\,h)$ type because it is located the closest to (3 1 0). All peak intensities were normalized to unity making it possible to analyze the shapes of the peaks.

Analysis of the data in Fig. 3b shows that the shape of the (2 2 2) reflection virtually does not change and corresponds to the instrumental resolution at all temperatures. The right shoulder of the (3 1 0) peak exhibits slight differences from the instrumental resolution even at high temperatures, which can be connected with the presence of the embryos of another phase. At $T = 259$ K (curve 3 in Fig. 3b), there are significant differences from the instrumental resolution near the 2θ values corresponding to the angular positions of the reflections of the tetragonal phase (the

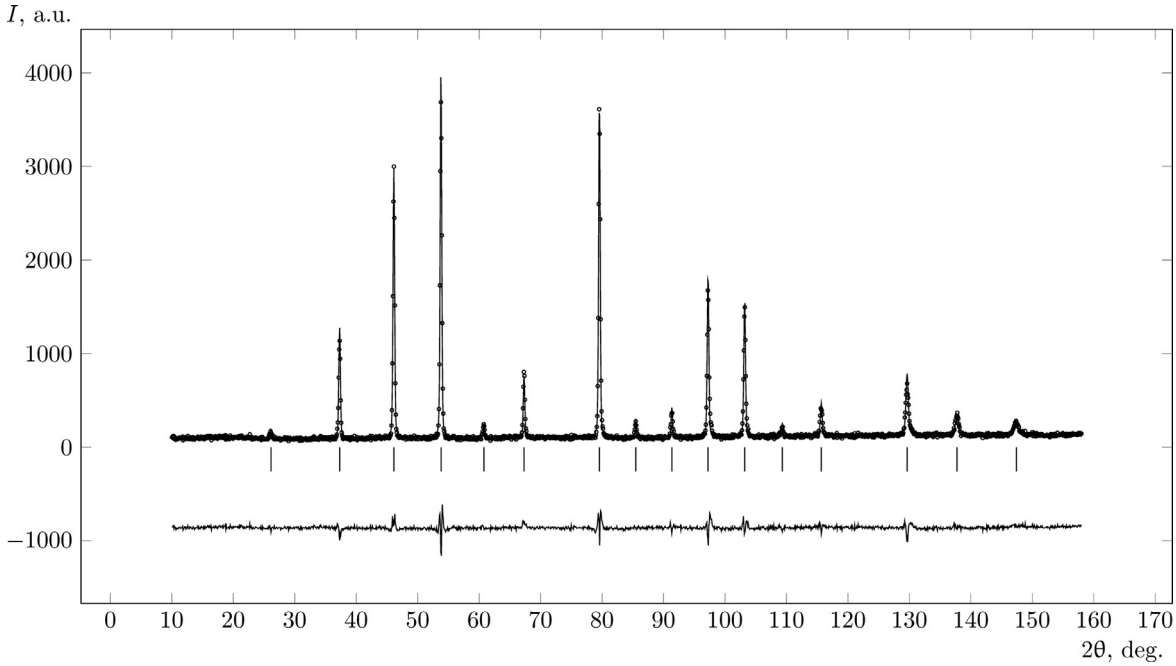

Fig. 2. Experimental at $T = 345$ K (dots) and calculated (line) diffraction spectra for (0.8)PFW–(0.2)PT. The vertical strokes mark the positions of the Bragg reflections of the calculated spectrum; the lower graph shows the residual between the approximation and the experimental data.

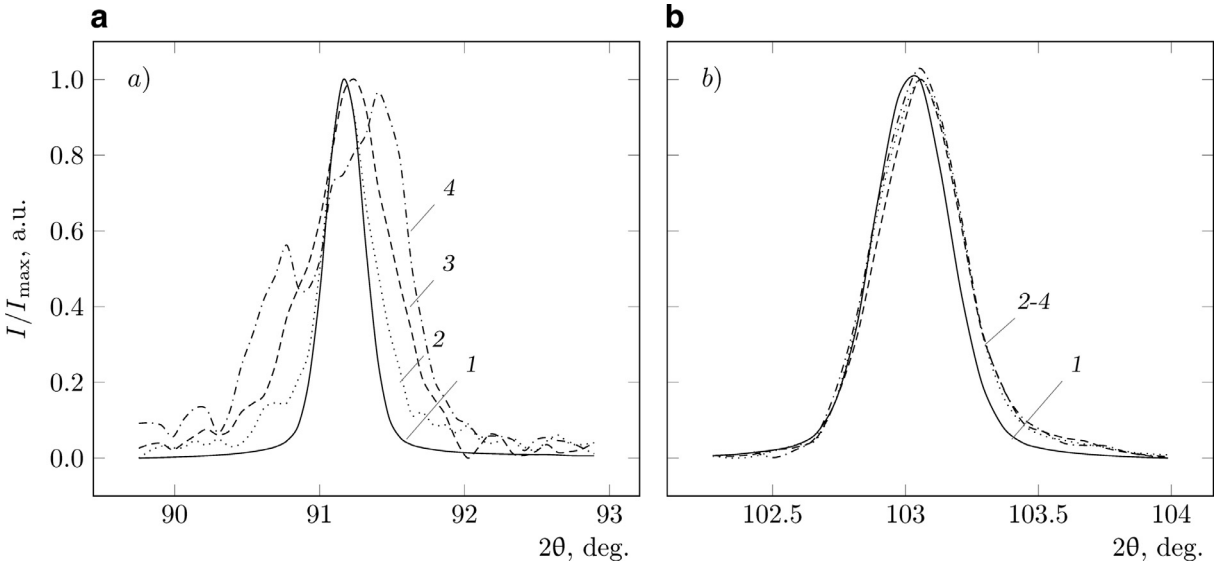

Fig. 3. Temperature evolution of the (3 1 0) (*a*) and the (2 2 2) (*b*) peaks of the diffraction spectrum of the solid (0.8)PFW–(0.2)PT solution: calculated instrumental profile (does not depend on temperature) (curve *1*); experimental spectra at $T = 287$ K (*2*), 259 K (*3*), 243 K (*4*).

decomposition of the reflections from the tetragonal and the cubic phases is shown in Fig. 4a).

Importantly, the observed effects for the distortion of the lineshape cannot be linked to the stresses caused by the defects that emerged while the sample was being fabricated, because, firstly, the tested samples were annealed, and, secondly, such stresses would have also manifested at high temperatures. Therefore, the most likely cause of the observed effects is the appearance of the tetragonal phase. This also explains the invariance of the lineshape of the ($h\,h\,h$) peaks at temperature decrease, as it is known that these peaks are not

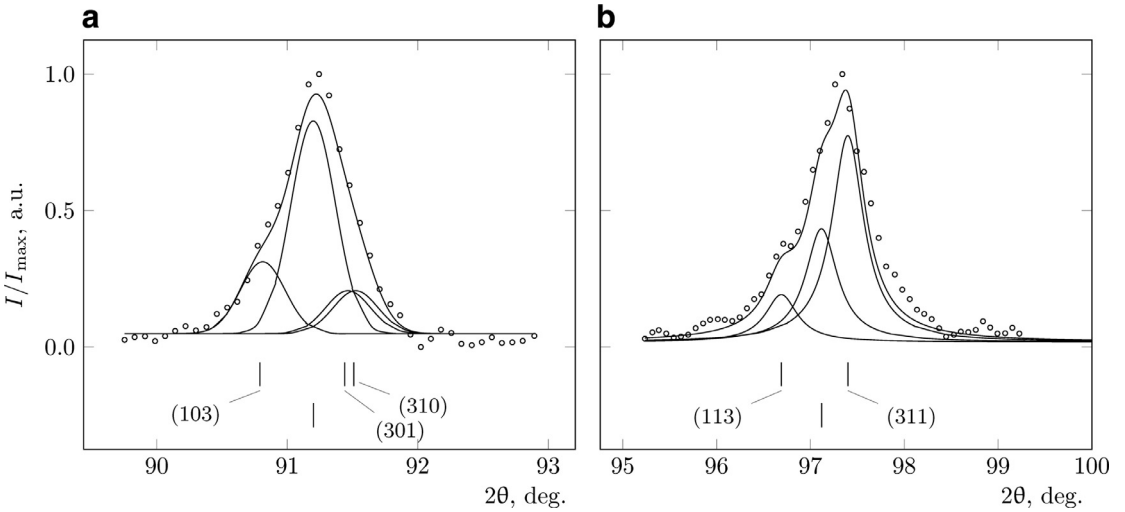

Fig. 4. Peaks of the experimental diffraction spectra (dots) of solid solutions decomposed into the contributions from the cubic and the tetragonal phases: *a* is the (3 1 0) peak for the (0.8)PFW–(0.2)PT compound; *b* is the (3 1 1) peak for the (0.7)PFW–(0.3)PT compound. The upper strokes mark the positions of the reflections of the tetragonal phase and the lower strokes those of the reflections of the cubic phase. $T = 259$ K (*a*) and 285 K (*b*).

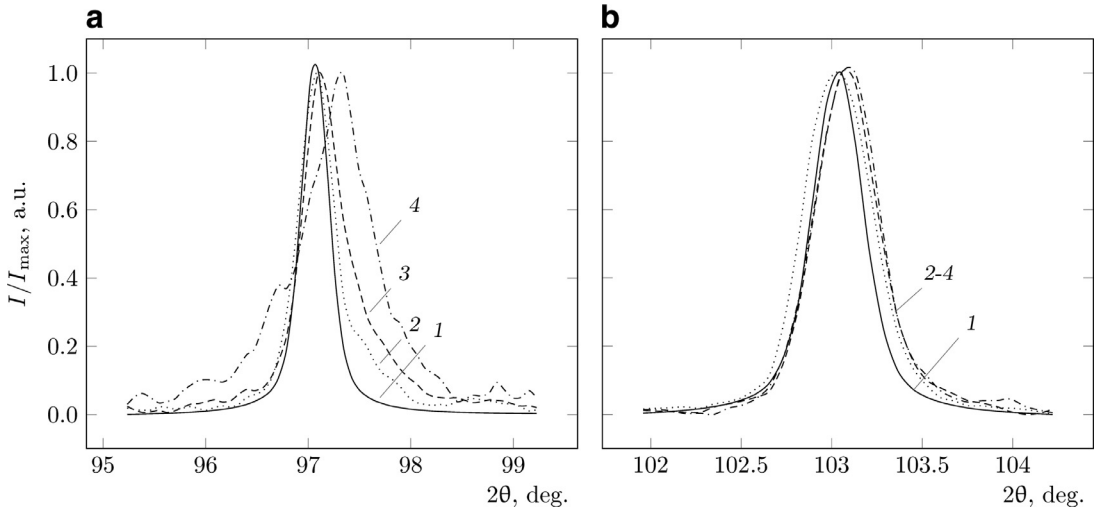

Fig. 5. Temperature evolution of the (3 1 1) (*a*) and the (2 2 2) (*b*) peaks of the diffraction spectrum of the solid (0.7)PFW–(0.3)PT solution: calculated instrumental profile (does not depend on temperature) (curve *1*); experimental spectra at $T = 395$ K (*2*), 335 K (*3*), 285 K (*4*).

split at the transition from the cubic to the tetragonal phase.

By refining the structure taking into account the presence of two phases, it was possible to achieve a reduction of *R*-factors (compared to the description within the cubic phase) and to adequately describe the profile of the experimental diffraction pattern $T = 259$ K. The contribution from the cubic phase does not disappear with the emergence of the contribution from the tetragonal phase, indicating that these two phases coexist.

In view of the above, we can conclude that at $T = 259$ K the sample with the composition $x = 0.2$ is in a two-phase state (tetragonal+cubic), and the phase transition starts in the temperature range $T = 259$–287 K.

Fig. 5 shows the temperature evolution of the (3 1 1) and (2 2 2) peaks for the sample with the composition $x = 0.30$, but at higher temperatures. As in the case of $x = 0.2$, the (2 2 2) reflection does not change its shape and virtually coincides with the instrumental resolution (see Fig. 5b). The (3 1 1) peak

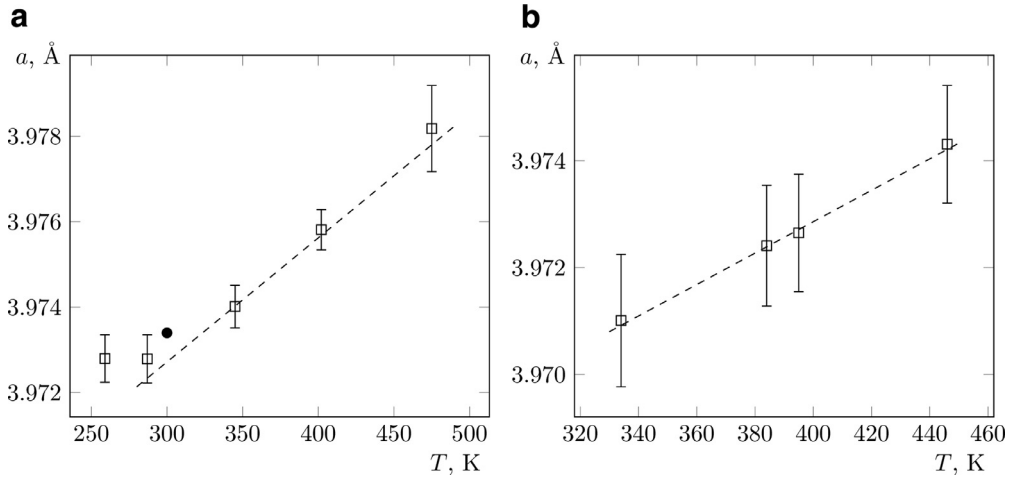

Fig. 6. The temperature dependence of the lattice parameters a for solid (1−x)PFW–(x)PT solutions for x=0.2 (a) and 0.3 (b). The dot marks the value of the parameter a at room temperature from Ref. [4].

has a deviation from the resolution function in the form of extended shoulders at large angles. These deviations exist even at high temperatures and increase under cooling. A possible cause for such deviations is similar to that described for the 0.2 composition.

At $T = 285$ K, there is a clear splitting of the (3 1 1) peak (Fig. 4b), but a small contribution from the cubic phase remains, which indicates the transition of the sample into the two-phase state. Subsequent full-profile analysis revealed that about 95% of the sample is in the tetragonal phase at this temperature.

Based on the above, we can conclude that the temperature at which the phase transition starts in the solid (1–x)PFW–(x)PT solution for $x = 0.3$ is in the 285–335 K range.

A full-profile analysis of the diffraction patterns was performed for the temperatures corresponding to the high-temperature cubic phase of the samples, refining the unit cell parameters, the coordinates of the atoms, and the thermal factors. The cubic lattice parameter for the samples with the $x = 0.2$ and 0.3 compositions increases linearly with temperature growth above room temperature (Fig. 6). The point in Fig. 6a is the value of the cell parameter $a = 3.9734$ Å at room temperature, taken from Ref. [4].

The analysis revealed that the model based on the perovskite structure yields anomalously high values of the Debye–Waller factor for lead. It is known that the lead ion is not in its (0, 0, 0) crystallographic position in lead-containing relaxors [9] and, in particular, in PFW [10]. Therefore, similar to [10], we used a model of the multiple-well potential where the lead is equiprobably displaced from the (0 0 0) position by a fixed distance in one of the 12 equivalent [1 1 0] directions. Fig. 7 and Table 1 show the values of these static displacements in the samples with the $x =$ 0, 0.20 and 0.30 compositions. It can be seen that the

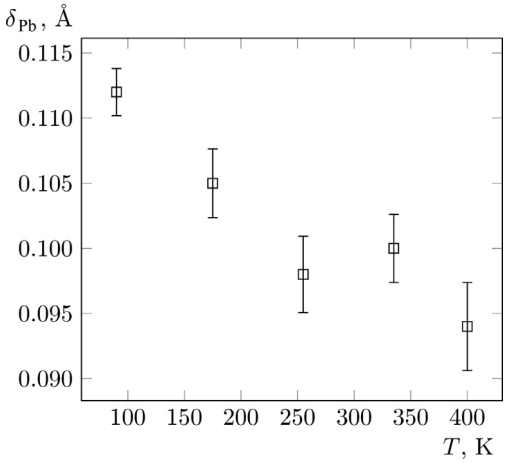

Fig. 7. Temperature dependence of the static displacements of lead atoms from the (0 0 0) position in PFW in solid (1–x)PFW–(x)PT solutions (see Table 1).

Table 1
Temperature dependence of the static displacements of lead atoms from the (0 0 0) position in solid (1–x)PFW–(x)PT solutions.

X	T (K)	δ_{Pb} (Å)
0.2	345	0.105 ± 0.002
	287	0.113 ± 0.002
	259	0.111 ± 0.002
0.3	395	0.076 ± 0.003
	335	0.082 ± 0.005

displacements decrease with an increase in $PbTiO_3$ concentration, which corresponds to the transition of PFW–PT from the relaxor state to the ferroelectric one, and is consistent with the dielectric spectroscopy data presented in Ref. [4].

Note that the values of the static displacements of lead ions for pure PFW that we obtained are in good agreement with those published in [10].

4. Conclusion

The structural studies that we carried out have established that the distortions of the lineshape of elastic reflections with the Miller indices different from $(h\,h\,h)$ are observed even at high temperatures for the $(1–x)$PFW–(x)PT compounds at $x = 0.2–0.3$. These distortions are likely connected with tetragonal distortions appearing in the high-temperature cubic phase. It has been found that at $T = 259$ K and 285, the solid solutions with the $x = 0.2$ and 0.3 composition, respectively, are in a two-phase state (the tetragonal + the cubic), with the tetragonal phase dominant.

We have obtained the temperature dependence of the lattice parameter of solid solutions for the values $x = 0$, 0.2 and 0.3, and have proved that the multiple-well potential model for lead ions can adequately describe the experimental data not only for pure PFW, but also for the solid $(1–x)$PFW–(x)PT solutions with the composition $x = 0.2$ and 0.3; the values of the lead displacements δ_{Pb} obtained through using this model amounted to approximately 0.1 Å.

The value of the static displacements was found to decrease with an increase in the concentration of lead titanate.

Acknowledgments

This study was supported by the Russian Science Foundation (Project no. 14-22-00136 ‘Structure and properties of self-organized and composite mesostructured ferroelectrics, piezoelectrics and multifunctional material’). The authors would also like to thank HZB for providing the opportunity to use the E9 neutron diffractometer.

References

[1] G.A. Smolenskiĭ, A.I. Agranovskaya, V.I. Isupov, New ferroelectrics of the complicated formula. III. Pb_2MgWO_6, $Pb_3Fe_2WO_9$ and Pb_2FeTaO_6, Solid State Phys. 1 (1) (1959) 990–992.

[2] V.A. Bokov, I.E. Mylnikova, G.A. Smolenskiĭ, Ferroelectric antiferromagnetics, JETP 15 (2) (1962) 643–646.

[3] V.P. Plakhtiĭ, E.I. Maltsev, D.M. Kaminker, Neytronograficheskoye issledovaniye nekotorykh soyedineniy so strukturoy perovskita [Neutronographic investigation of some perovskite-structured compounds], Izv. AN SSSR 28 (2) (1964) 436–439.

[4] L. Feng, Z.G. Ye, Phase diagram and phase transitions in the relaxor ferroelectric $Pb(Fe_{2/3}W_{1/3})O_3$–$PbTiO_3$ system, J. Solid State Chem. 163 (2) (2002) 484–490.

[5] S.S. Levina, N.P. Parashchukov, Issledovaniye segnetomagnitnykh tverdykh rastvorov sistemy $Pb(Fe_{2/3}W_{1/3})O_3$–$PbTiO_3$ [Study of magnetoelectric solid solutions $Pb(Fe_{2/3}W_{1/3})O_3$-$PbTiO_3$], Izv. vuzov. Fizika 1972 (8) (1972) 131–133.

[6] L. Mitoseriu, P.M. Vilarinho, J.L. Baptista, Phase coexistence in $Pb(Fe_{2/3}W_{1/3})O_3$–$PbTiO_3$ solid solutions, Appl. Phys. Lett. 80 (23) (2002) 4422–4424.

[7] K. Okadzaki, Tekhnologiya keramicheskikh dielektrikov [Ceramic dielectrics technology], Per. s yapon., Moscow, Energiya, 1976.

[8] J. Rodriguez-Carvajal, Program FULLPROF https://www.ill.eu/sites/fullprof/.

[9] S. Vakhrushev, S. Zhukov, G. Fetisov, V. Chernyshov, The high-temperature structure of lead magnoniobate, J. Phys. Condens. Matter 6 (22) (1994) 4021–4027.

[10] S.A. Ivanov, S.G Eriksson, R. Tellgren, H. Rundlöf, Neutron powder diffraction study of the magnetoelectric relaxor $Pb(Fe_{2/3}W_{1/3})O_3$, Mater. Res. Bull. 39 (14–15) (2004) 2317–2328.